MAGNETIC FIELD SIMULATIONS IN FLYWHEEL ENERGY STORAGE SYSTEM WITH SUPERCONDUCTING BEARING

Asma SAMOH[1], Chitnarong SIRISATHITKUL[2], Sampart CHEEDKET[3], Sorasak DANWORAPHONG[4]

Magnetic fields between a permanent magnetic flywheel ring and a superconducting bearing are simulated using COMSOL Multiphysics and compared to analytical results. The flux distribution around a Neodymium Iron Boron ring of 20 mm in inner radius, 80 mm in outer radius, and 23 mm in thickness can be visualized and compared in radial and axial directions. The flux density simulated along the angular direction at the outer radius is 0.34-0.14 T at 5-20 mm away from the ring. Furthermore, the flux exclusion by the superconducting bearing required for lifting flywheel rings of different geometries are demonstrated.

Keywords: COMSOL Multiphysics, flywheel energy storage, permanent magnetic ring, superconducting bearing, magnetic flux density

1. Introduction

Flywheel energy storage systems (FESS) have been under research and development to retrieve the dispensed energy for subsequent uses. The electrical input accelerates the flywheel by using the built-in motor and return the electrical energy by using this same motor as a generator. With this operation, energy is stored in forms of the rotation of flywheel ring. Their operations have long cycle life and minimal environment footprint [1]. Such devices are currently implemented in wind turbine generators [2] and power systems [3]. Like electromagnetic regenerative shock absorbers [4], it can be employed in vehicles [1]. Either mechanical or magnetic bearings are employed to minimize the friction. Without mechanical contact, the latter is attractive for its low loss and maintenance cost. A high speed (up to 40,000 rpm) and energy storage (around 10 MJ) FESS was built with magnetic bearings [5].

[1] Graduate student, Division of Physics, School of Science, Walailak University, Nakhon Si Thammarat, Thailand, e-mail: iamasma62@gmail.com
[2] Assoc. Prof., Division of Physics, School of Science, Walailak University, Nakhon Si Thammarat, Thailand, e-mail: chitnarong.siri@gmail.com
[3] Lecturer, Division of Physics, School of Science, Walailak University, Nakhon Si Thammarat, Thailand, e-mail: sampart@gmail.com
[4] Assoc. Prof., Division of Physics, School of Science, Walailak University, Nakhon Si Thammarat, Thailand, e-mail: dsorasak@gmail.com

Magnetic levitation has been analysed by using different approaches [6-13] and substantial repulsive forces due to Meissner effect in high temperature superconductors have found applications in rail transportation, motor/generator as well as FESS [13-15]. Interactions between superconducting bearings and permanent magnets have been simulated in 2D and 3D models using the finite element method [14,15]. Magnetic flux density and repulsive force were studied on different magnetic flywheels including an array of small magnets [16] and a three-magnet multi-surface system [17]. In addition to permanent magnetic flywheels, superconducting bearings have been used with superconducting flywheels [18,19]. The levitation force differs with the variation in materials and geometry. Such variations lead to a variety of FESS applications ranging from miniature devices to high power storage [20].

This report aims to analyze the magnetic flux distribution between flywheel rings with superconducting bearing for storing excess energy in machinery in forms of the kinetic energy. The hollow cylindrical shape is commonly produced and implemented in the rotation. Various cylindrical magnets including the Halbach geometry have been used for generating magnetic field with high efficiency [21]. However, the previous implementations in flywheel concentrate on the simulation of levitation force as a function of the distance. Moreover, the appropriate dimensions of the permanent magnetic flywheel ring in each system still requires the investigation for comparison with the flux from superconducting coils [18,19]. The magnetic field analysis in this report is useful for optimizing the design of novel miniature devices for energy harvesting and storage.

2. Methodology

As shown by the diagram in Fig.. 1, the energy storage system in a vacuum chamber is composed of a permanent magnetic flywheel ring, superconducting bearings and motor/generator. Neodymium Iron Boron is selected as a permanent magnet since its remanent flux density is commonly 1.3 T. The geometry of this flywheel ring is varied into three series as listed in Table 1.

Table 1

Three variations in height (*H0*), inner radius (*Ri*) and outer radius (*Ro*) of the permanent magnetic flywheel rings used in the simulation.

Series	*H0* (mm)	*Ri* (mm)	*Ro* (mm)
1	23.0	20.0	80.0
2	11.5	20.0	80.0
3	23.0	20.0	53.0

Whereas the height and radius of the flywheel differ in this study, the dimensions of superconducting Yttrium Barium Copper Oxide bearing are fixed with the height, inner and outer radii of 5, 20 and 80 mm, respectively.

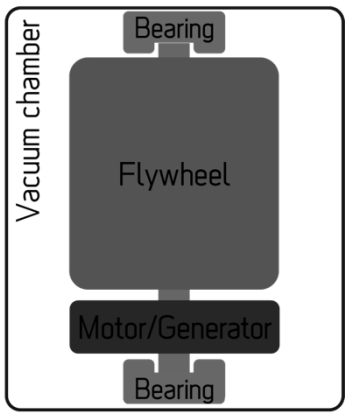

Fig. 1 Components of flywheel energy storage systems.

Numerical simulations were carried out by finite element method using COMSOL Multiphysics version 5.2 program [22]. COMSOL has successfully been used to simulate a variety of devices [15,23-25]. In this work, free triangular elements were implemented in 2D axisymmetric for a half of model. The magnetic flux density (**B**) generated by the magnetic flywheel ring was computed from the magnetic vector potential (**A**).

$$\mathbf{B} = \nabla \times \mathbf{A} \tag{1}$$

with the boundary condition;

$$\mathbf{n} \times \mathbf{A} = 0 \tag{2}$$

where **n** is the outward normal vector.

Variations in the magnetic flux density with its geometry and the presence of the superconducting bearing was displayed. Moreover, the axial and radial components of the magnetic flux density were plotted as functions of the distance and angle.

3. Results and Discussions

A profile of magnetic flux density exemplified in Fig. 2 is generated by the flywheel ring of 20 mm in inner radius, 80 mm in outer radius and 23 mm in thickness (Series 1). Magnetic field lines and directions are varied corresponding to the contour lines and vectors, respectively. Colors represent the magnetic flux density ranging from red (the highest) to blue (the lowest). The magnetic flux is

concentrated on both right and left edges of the flywheel ring. The magnetic flux density is predictably reduced in areas away from the magnet, displayed as the blue zone. Inside the flywheel ring, magnetic field direction is rather constant as shown by parallel magnetic field lines but its magnitude is varied as discussed in Figs. 3-4.

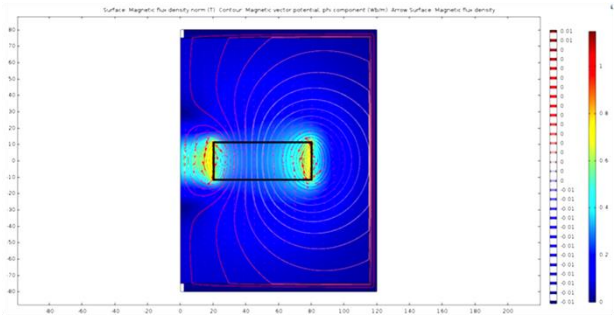

Fig. 2. Profile of magnetic flux density generated by the flywheel ring (Series 1).

The axial (z) and radial (r) components of magnetic flux density are plotted as a function of distance from the center in Fig. 3. The z-component is maximum at the center of the ring and approaches zero with the increasing distance away from the surface. The flux density switches its sign, from negative to positive, around the inner radius and the flux density becomes rather constant from 30 to 60 mm. By contrast, the r-component of magnetic flux density is approximately zero at the center of the ring and reaches the maximum at the inner radius. The flux density then monotonically rises with the increasing distance as the field lines switch their sign to positive. The magnetic flux density is maximum at the outer radius consistent with the right edge in Fig. 2. Such variations are similar in all four displacements from the surface (Z = 5, 10, 15, and 20 mm) compared in Fig. 3 with the decrease in magnitude away from the surface. The magnetic flux density in both, z- and r-direction, can also be analytically found. Given a constant magnetization, magnetic flux density is independent of induced current density. The induced surface current density is the only term contributing to the flux density. The solution can be found in terms of elliptical integral of first, $K\left(k\left(r,z\right)\right)$ second, $E\left(\mathrm{k}\left(r,z\right)\right)$ and third kind, $Pi\left(g\left(r\right),k\left(r,z\right)\right)$. The flux density, r- and z- component, can be written in terms of *r* and *z* as;

$$B_r = \frac{B_0}{\pi}\sum_{n=0}^{1}\sum_{m=0}^{1}(-1)^{n+m}\frac{R_n}{\sqrt{H_{nm}\left(r,z\right)}}\left[\frac{1}{k\left(r,z\right)}\left(k\left(r,z\right)-2\right)K\left(k\left(r,z\right)\right)+2E\left(k\left(r,z\right)\right)\right] \tag{3}$$

$$B_z = \frac{B_0}{\pi}\sum_{n=0}^{1}\sum_{m=0}^{1}(-1)^{n+m}\frac{R_n}{\sqrt{H_{nm}(r,z)}}\frac{Z_m(z)}{\left(D_m(r)\right)^2}\times \left[\left(R_n+\frac{r}{R_m}-\frac{2\left(\frac{r}{R_m}\right)}{g(r)}\right)Pi\left(g(r),k(r,z)\right)+\frac{2\left(\frac{r}{R_m}\right)}{g(r)}K\left(k(r,z)\right)\right] \quad (4),$$

where B_0 is magnetic flux density due to magnetization, given as 1.3 T.

R_a is the average value of inner, R_i and outer, R_o radius and R_n is $1+(-1)^n\frac{\frac{R_o-R_i}{2}}{R_a}$.

$Z_m(z)$ is $\frac{z}{R_a}+(-1)^m\left(\frac{h}{R_a}\right)$.

$H_{nm}(r,z)$ is expressed as $\left(\frac{r}{R_a}\right)^2+(R_n)^2+\left(Z_m(z)\right)^2+2\left(\frac{r}{R_a}\right)R_n$ while

$D_n(r)$ is $\frac{r}{R_a}+R_n$. $g(r)$ is $\frac{4\left(\frac{r}{R_a}\right)R_n}{\left(D_n(r)\right)^2}$ and $k(r,z)$ is $\frac{4\left(\frac{r}{R_a}\right)R_n}{H_m(r,z)}$.

By substituting all known variables, i.e., thickness, inner and outer radius, remanant flux density, the flux density evaluated by Equations (3) and (4) in both directions are in good agreement with those simulated by the finite difference method, as shown in Figs. 3 (a), (b), (c), and (d).

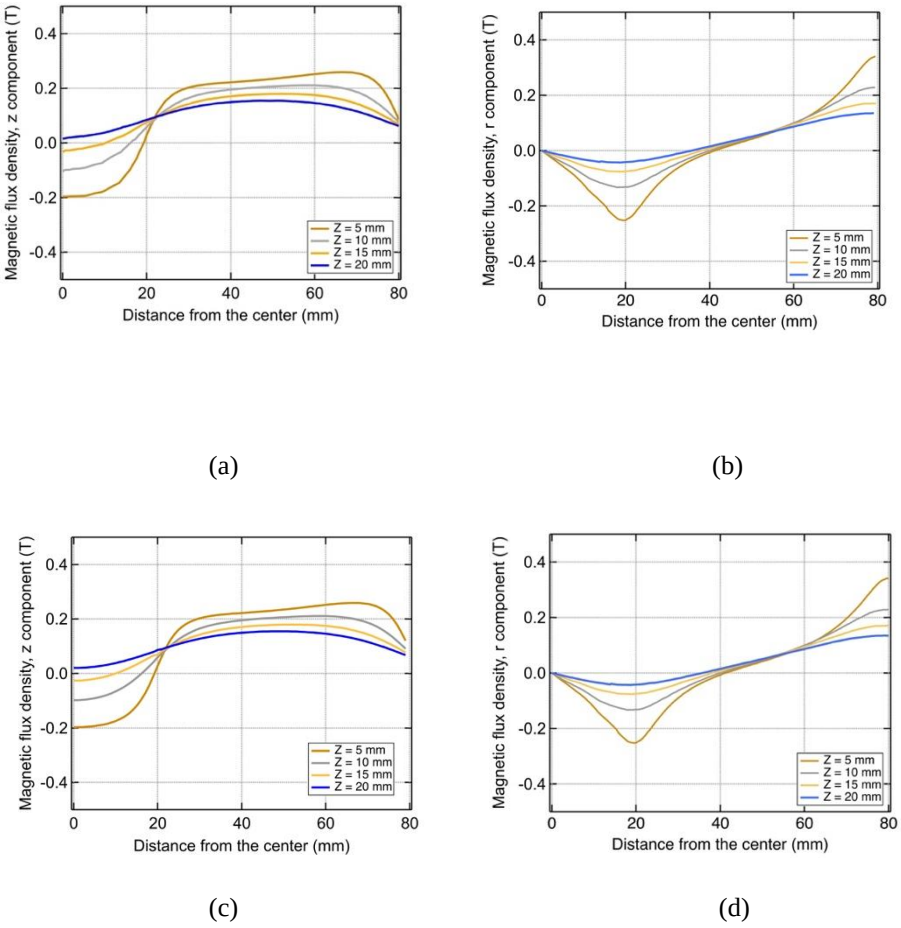

Fig. 3. Magnetic flux density of the flywheel ring in (a) z-component and (b) r-component simulated along the radial direction from the center to the right side of the ring. (c) and (d) represent the magnetic flux density analytically determined by Equations 3 and 4.

Since the system possesses azimuthal symmetry, both components of magnetic flux density are angularly constant for each height (z) as shown in Fig. 4. This numerical simulation is also in accordance with the analytical result by the modified critical state model [7]. Furthermore, the simulated fields by COMSOL are also comparable to the measurement of magnetic field from Neodymium Iron Boron disk of 12.7 mm in both diameter and thickness [11], indicating that this magnetic ring can be used in the flywheel energy storage system.

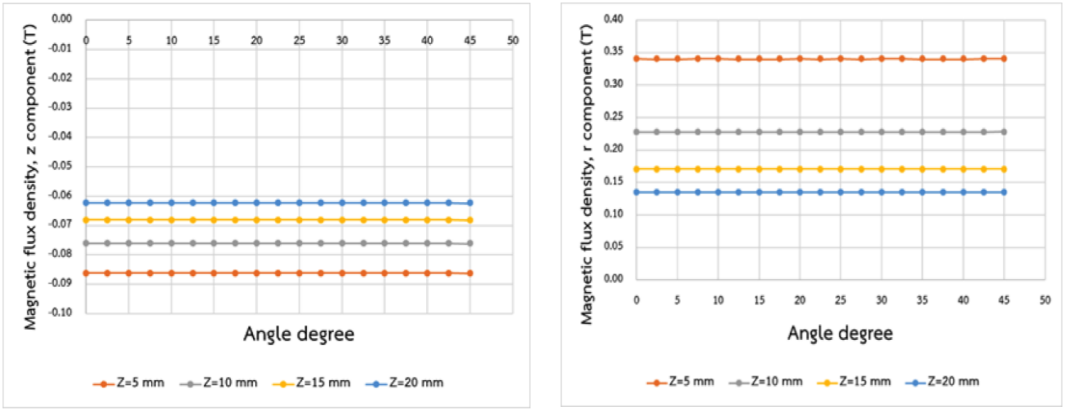

(a) (b)

Fig. 4. Magnetic flux density of the flywheel ring in (a) z-component and (b) r-component measured along the angular direction at radius 80 nm. Four different displacements from the surface (Z = 5, 10, 15, and 20 mm) are compared.

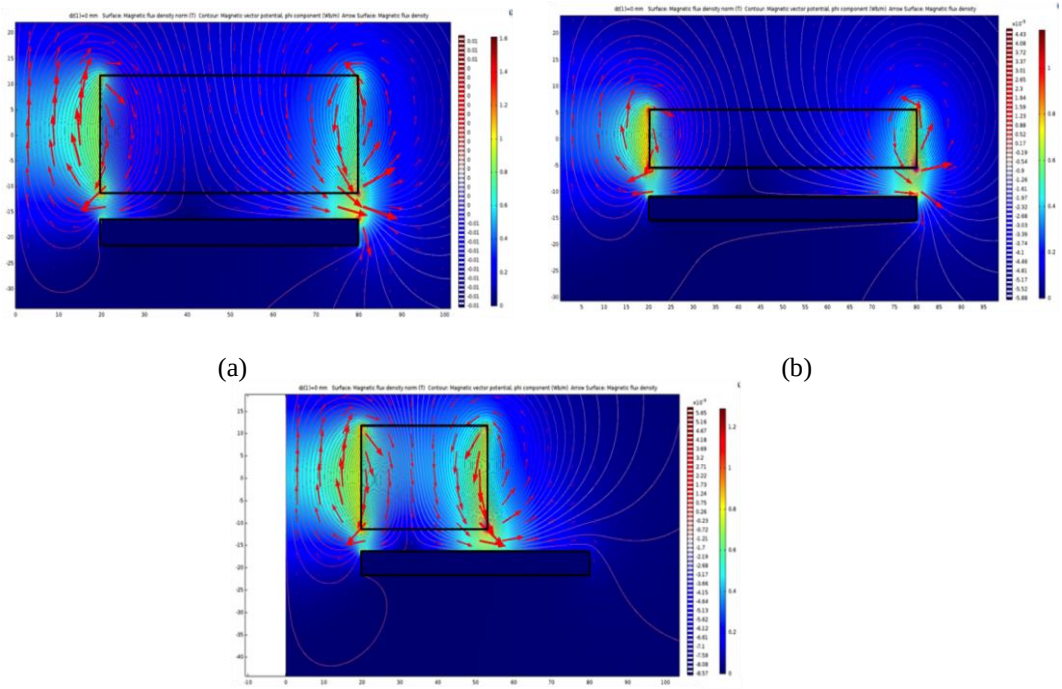

(a) (b)

(c)

Fig. 5. Profiles of magnetic flux density of the magnetic flywheel rings ((a) Series 1, (b) Series 2, (c) Series 3) at 5 mm displacement above the superconductor bearing.

Spatial distributions of magnetic flux density shown in Fig. 5, demonstrate interaction between the magnetic flywheel ring and the superconducting bearing. For all three series, the magnetic flux remains concentrated on both left and right sides of the flywheel. The effect of the superconducting bearing is demonstrated as the surrounding magnetic flux is repelled. Such magnetic flux profile creates the levitation force acting on the flywheel ring for practical energy harvesting and storage devices. For a different configuration with switching positions of a superconductor and a permanent magnet, Zheng recently used COMSOL to simulate levitation and guidance force acting on a floating superconducting disk above the permanent magnetic guideway [25]. Despite the size difference, the magnetic flux density away from the permanent magnets exhibit a similar trend to that observed in Fig. 3(a).

4. Conclusions

Magnetic flux density distribution from a Neodymium Iron Boron magnetic ring of 20 mm in inner radius, 80 mm in outer radius, and 23 mm in thickness with a remanent magnetic flux density of 1.3 T was initially simulated with COMSOL Multiphysics program. Along the angular direction from 0°-45°, both axial and radial components of magnetic flux densities are uniform. As shown in Fig. 4(a), the z-component of magnetic flux density is between -0.09 T and -0.06 T when the displacement from the ring surface is 5-20 mm. The r-component is much higher with the maximum close to 0.35 T in the case of 5 mm from the surface. This implies that one can use such magnetic ring for energy storage when levitated at large displacements. This numerical simulation was consistent with the analytical method. Simulations then demonstrated the interaction of flywheel rings of three varying sizes with an Yttrium Barium Copper Oxide superconducting ring of 20 mm in inner radius, 80 mm in outer radius, and 5 mm in thickness. The result from this unique geometry indicates that the repulsive force useful for stable flywheel energy storage systems can be obtained in practical use of miniature devices.

REFERENCES

[1] *M. Hedlund, J. Lundin, J. Santiago, J. Abrahamsson and H. Bernhoff*, "Flywheel Energy Storage for Automotive Applications", in Energies, **vol. 8**, 2015, pp. 10636–10663

[2] *R. Sebastian and R. P. Alzola*, "Flywheel Energy Storage Systems: Review and Simulation for an Isolated Wind Power System", in Renewable and Sustainable Energy Reviews, **vol. 16**, 2012, pp. 6803–6813

[3] *A. K. Arani, H. Karami, G. B. Gharehpetian and M.S.A. Hejazi*, "Review of Flywheel Energy Storage Systems Structures and Applications in Power Systems and Microgrids", in Renewable and Sustainable Energy Reviews, **vol. 69**, 2017, pp. 9–18

[4] *A.-L. Cătănescu and T. Ion*, "Analysis of Electromagnetic Regenerative Shock Absorber", in University Politehnica of Bucharest Scientific Bulletin Series C, **vol. 77**, 2015, pp. 297–304

[5] *A. Mystkowski and A. Rowiński*, "Construction and Control of AMBs High Speed Flywheel", in Archive of Mechanical Engineering, **vol. 58**, 2011, pp. 79–89

[6] *D. Camacho, J. Mora, J. Fontcuberta and X. Obradors*, "Calculation of Levitation Forces in Permanent Magnet-Superconductor Systems Using Finite Element Analysis", in Journal of Applied Physics, **vol. 82**, 1997, pp. 1461–1468

[7] *Z. J. Yang*, "Levitation Forces on a Permanent Magnet Over a Superconducting Plane: Modified Critical-State Model", in Journal of Superconductivity, **vol. 10**, 1997, pp. 137–149

[8] *A. Azzouza, H. Allag, J.-P. Yonnet and P. Tixador*, "3-D New Calculation Principle of Levitation Force Between Permanent Magnet and Hard Type-II Superconductor Using Integral Approach", in IEEE Transactions on Magnetics, **vol. 53**, 2017, article no. 8109705

[9] *F. Y. Alzoubi*, "Analysis of the Interaction Between Magnet and Superconducting Ring in the Mixed State", in Indian Journal of Pure & Applied Physics, **vol. 53**, 2015, pp. 416–419

[10] *M. K. Alqadi, F. Y. Alzoubi, S. M. Saadeh, H. M. Al-Khateeb and N.Y. Ayoub*, "Force Analysis of a Permanent Magnet and a Superconducting Hollow Cylinder", in Journal of Superconductivity and Novel Magnetism, **vol. 25**, 2012, pp. 1469–1473

[11] *A. Cansiz*, "Vertical, Radial and Drag Force Analysis of Superconducting Magnetic Bearings", in Superconductor Science and Technology, **vol. 22**, 2009, article no. 075003

[12] *I. V. Nemoianu and E. Cazacu*, "Quasi-Vertical Permanent Magnet Levitation: Analytical Model and Characterization", in Revue Roumaine des Sciences Techniques: Série Électrotechnique et Énergétique, **vol. 59**, 2014, pp. 13–24

[13] *A. Morandi, M. Fabbri, P. L. Ribani, A. Dennis, J. Durrell, Y. Shi and D. Cardwell*, "The Measurement and Modeling of the Levitation Force Between Single-Grain YBCO Bulk Superconductors and Permanent Magnets", in IEEE Transactions on Applied Superconductivity, **vol. 28**, 2018, article no. 3601310

[14] *L. Quéval, K. Liu, W.-J. Yang, V. M. R. Zermeño and G. T. Ma*, "Superconducting Magnetic Bearings Simulation Using an H-Formulation Finite Element Model", in Superconductor Science and Technology, **vol. 31**, 2018, article no. 084001

[15] *J. Zheng, H. Huang, S. Zhang and Z. Deng*, "A General Method to Simulate the Electromagnetic Characteristics of HTS Maglev Systems by Finite Element Software", in IEEE Transactions on Applied Superconductivity, **vol. 28**, 2018, article no. 3600808

[16] *M. Ikeda, A. Wongsatanawarid, H. Seki and M. Murakami*, "Interaction of Bulk Superconductors with Flywheel Rings Made of Multiple Permanent Magnets", in Physica C: Superconductivity and Its Applications, **vol. 469**, 2009, pp. 1270–1273

[17] *S. Sivrioglu, S. Basaran and A. S. Yildiz*, "Multisurface HTS-PM Levitation for a Flywheel System", in IEEE Transactions on Applied Superconductivity, **vol. 26**, 2016, article no. 3603206

[18] *K. Nagashima, H. Seino and N. Sakai*, "Superconducting Magnetic Bearing for a Flywheel Energy Storage System Using Superconducting Coils and Bulk Superconductors", in Physica C: Superconductivity and Its Applications, **vol. 469**, 2009, pp. 1244–1249

[19] *Y. Arai, H. Seino, K. Yoshizawa and K. Nagashima*, "Development of Superconducting Magnetic Bearing with Superconducting Coil and Bulk Superconductor for Flywheel Energy Storage System", in Physica C: Superconductivity and Its Applications, **vol. 494**, 2013, pp. 250–254

[20] *Y. Miyazaki, K. Mizuno, T. Yamashita, M. Ogata, H. Hasegawa, K. Nagashima, S. Mukoyama, T. Matsuoka, K. Nakao, S. Horiuch, T. Maeda and H. Shimizu*, "Development

of Superconducting Magnetic Bearing for Flywheel Energy Storage System", in Cryogenics, **vol. 80**, 2016, pp. 234–237

[21] *R. Bjork*, "The Magnetic Properties of Hollow Cylindrical Ideal Magnet", in Journal of Magnetism and Magnetic Materials, **vol. 416**, 2016, pp. 321-324

[22] COMSOL AB, Tegn´ergatan 23, SE-111 40 Stockholm, Sweden.

[23] *R. Djekidel, M. Djilali and C. Hadjad*, "Assessment of Magnetic Induction Emission Generated by an Underground HV Cable", in University Politehnica of Bucharest Scientific Bulletin Series C, **vol. 78**, 2016, pp. 179–184

[24] *F. Dragomir, I. A. Ivan, I. V. Gurgu, N. G. Radulescu, I. A. Bucurica and I. D. Dulama*, "COMSOL Simulation of Electromagnetic Field Required for a Microrobot Actuation", in Journal of Science and Arts, **vol. 18**, 2018, pp. 523–529

[25] *J. Zheng, H. Huang, S. Zhang and Z. Deng*, "A General Method to Simulate the Electromagnetic Characteristics of HTS Maglev Systems by Finite Element Software", in IEEE Transactions on Applied Superconductivity, **vol. 28**, 2018, article no. 3600808